Sub-surface intensification of marine heatwaves off southeastern Australia: the role of stratification and local winds.

A. Schaeffer[1] and M. Roughan[1]

Amandine Schaeffer, schaeffer.amandine.uni@gmail.com

[1]Coatal and Regional Oceanography Lab,

School of Mathematics and Statistics,

UNSW Australia, Sydney NSW 2052

Accepted Article

This article has been accepted for publication and undergone full peer review but has not been through the copyediting, typesetting, pagination and proofreading process, which may lead to differences between this version and the Version of Record. Please cite this article as doi: 10.1002/2017GL073714

©2017 American Geophysical Union. All Rights Reserved.

Abstract. Marine heatwaves (MHWs) are becoming more common with record events occurring around the world, and unprecedented biological impacts including mass mortality and habitat shifts. However, little is known about the statistical characteristics of MHWs due to the lack of long term in situ observations. Using two historical datasets spanning 1953 (and 1992) to 2016 we use a seasonally-varying climatology and temperature anomalies to identify and characterize MHW events down to 100 m depth in coastal waters off southeastern Australia. We show that MHWs regularly extend the full depth of the water column, with a maximum intensity below the surface. Extreme temperatures at depth are driven by local downwelling favorable winds that mix the water column and reduce the stratification. These results show the importance of considering sub-surface hydrography, and that sea surface temperature is insufficient to fully understand MHWs which are having disastrous ecological consequences in coastal regions globally.

Keypoints:

- We present the 1st sub-surface analysis of coastal MHWs (marine heatwaves) using a 60+ year dataset
- MHWs regularly extend to the sea floor, mostly during weak stratification driven by downwelling winds
- MHWs are most intense at depth, indicating a pressing need for more sub-surface temperature records

Accepted Article

©2017 American Geophysical Union. All Rights Reserved.

1. Introduction

Marine heatwaves (MHWs), defined as "discrete prolonged anomalously warm water events" [*Hobday et al.*, 2016], are having disastrous effects on the ocean ecosystems around the world. Over the last 30 years, extremely hot sea surface temperatures (SSTs) have become more common in 1/3rd of the world's coastal areas [*Lima and Wethey*, 2012]. In response to the unusual thermal stress, marine communities have to either acclimatize or track more suitable habitat further poleward or deeper. This includes not only shallow communities, but also benthic species, some coral communities and seaweed below the surface mixed layer (SML). Increasingly habitat forming species are dying, and are not able to recover after the MHW has subsided [*Wernberg et al.*, 2016]. Unfortunately, little is known about temperature extremes at depth due to the lack of long-term in situ measurements.

Around Australia, the most severe MHW event in 140 years occurred during the Austral summer (2010/2011) off Western Australia, lasting over a month, with anomalies up to 5 ^{o}C above the climatological mean [*Pearce and Feng*, 2013]. It led to large seagrass, fish and invertebrate mortality [*Pearce and Feng*, 2013; *Thomson et al.*, 2015] and a poleward shift of tropical species [*Wernberg et al.*, 2013]. A survey 2 years later showed a 43% loss of kelp forests along the coast (28-34 ^{o}S) with a community-wide shift toward warm water seaweeds and fish [*Wernberg et al.*, 2016].

On different occasions, MHWs also affected ecosystems on the Great Barrier Reef on the east coast of Australia, where declines in coral cover, fish diversity and habitat were observed and attributed to extreme temperatures (*Johnson* [2014] and references herein).

Accepted Article

©2017 American Geophysical Union. All Rights Reserved.

Further south, *Verges et al.* [2016] showed evidence of tropicalization of fish communities in temperate regions, in particular fish herbivory consuming kelp, leading to a decline of the kelp habitat. In cold temperature regions (Tasmania), increasing ocean temperatures and the extension of the southward flowing East Australian Current led to a poleward range extention of many species of fish [*Last et al.*, 2011] and habitat destroying sea urchin [*Ling et al.*, 2009], leading to a massive loss of kelp [*Johnson et al.*, 2011].

MHWs can be driven by atmospheric conditions, with an increase in air temperature, weak wind stress and an overall decreased upward air-sea heat flux [*Bond et al.*, 2015; *Chen et al.*, 2015]. They have also been linked to mesoscale ocean circulation advecting heat and temperature extremes, superimposed on interranual climate variability. For instance, for the 2011 Western Australia event, it was shown that the Leeuwin current contributed to 2/3 of the ocean temperature changes, while heat fluxes explained the remaining 1/3 [*Benthuysen et al.*, 2014]. The anomalous warm-water transport of the Leeuwin current was linked with near record La Nina conditions [*Feng et al.*, 2013]. The boundary current along the east coast, the East Australian Current, also influences temperature extremes. *Oliver et al.* [2014] showed a projected hotspot corresponding to the East Australian Current separation region in response to increased eddy activity. These anomalously warm temperatures are projected to increase by up to 4^{o}C over 50 years, with a maximum increase located 500 km south of the maximum increase in mean SST [*Oliver et al.*, 2014]. This different spatial pattern between the increase of mean and extreme temperature shows that in situ ocean warming is not the only driver for the intensification of MHWs, and that ocean dynamics should be considered when trying to

Accepted Article

©2017 American Geophysical Union. All Rights Reserved.

understand these extreme events.

Despite the devastating ecological impacts of MHWs, few studies have investigated temperature extremes below the surface. Satellite SST has revealed the spatial extent of MHWs at reasonable spatial and temporal resolution (O(km, day), *Scannell et al.* [2016]). However SST may do little to inform the impact on benthic or pelagic marine communities that live below the surface. Using temperature data from Argo floats, *Feng et al.* [2013] showed that the temperature anomalies in the deep ocean were constrained to the SML during the 2011 MHW event. However, in situ measurements on the shelf showed a consistent temperature increase over depth down to 200 m. Furthermore *Pearce and Feng* [2013] showed several occasions when temperature extremes were well-mixed to the seafloor at 100 m depth (see Fig. 5 in *Pearce and Feng* [2013]). Since temperature extremes can affect shelf areas far deeper than the SML, more research on the vertical structure of MHWs is needed particularly in coastal regions.

More specifically, some of the key questions that remain unclear are: Do MHWs extend to sea bed on continental shelves, and if yes, how often? Are temperature anomalies more intense at depth or at the surface? Is SST a good proxy for the MHW duration and intensity? Should we expect similar characteristics and seasonality below the SML?

In this study we use 2 long-term independent in situ dataset on the southeastern (SE) Australian continental shelf off Sydney (34 ^{o}S). The region is strongly influenced by the East Australian Current eddy field [*Schaeffer et al.*, 2013, 2014b], and identified as an ocean warming hotspot [*Cai et al.*, 2005; *Wu et al.*, 2012; *Sen Gupta et al.*, 2015; *Oliver et al.*, 2014]. These temperature measurements enable us to generate a daily climatology,

©2017 American Geophysical Union. All Rights Reserved.

Accepted Article

which we use to identify and investigate temperature extremes throughout the water column. We discuss our results in the context of forcing mechanisms, intensity and the urgent need for sub surface temperature observations.

2. Datasets and methods

2.1. In situ temperature observations

Around Australia, long-term sampling of the ocean temperature has been conducted at 3 sites, since the 1940-50s [*Thompson et al.*, 2009] including Port Hacking off Sydney (PH100, depth of ∼110 m, 34^{o}S, subtropical zone). Historical bottle sampling spanned the period 1953-2009, with weekly to monthly observations nominally at depths of 0, 10, 20, 30, 40, 50, 75 and 100 m, with some variation in depth over time (Fig. 1b). In 2009, in the framework of the Integrated Marine Observing System (IMOS), PH100 was chosen as a national reference station (NRS), together with 9 other sites around Australia [*Lynch et al.*, 2014]. Since then, biogeochemical samples were combined with monthly CTD casts from the surface to 100 m. In addition, a mooring was installed (34.12^{o}S, 151.22^{o}E) in October 2009, instrumented with 10 AQUA logger 520T that measure water temperature every 5 min at 8 m intervals from the sea floor to approximately 17 m from the surface. PH100 is the only site in the country where a mooring with good vertical resolution matches the location of long-term samplings.

A second coastal mooring is located 26 km to the north of the PH100 site, maintained by Sydney Water Corporation since November 1990 in 65 m of water, called the Ocean Reference Station (ORS065, 33.90^{o}S, 151.32^{o}E, Fig. 1a). It is located less than 3 km from the shore and initially included a surface expression and real-time capability (prior to 2006). Hourly temperature time-series were obtained from 2 thermistors just below the

©2017 American Geophysical Union. All Rights Reserved.

Accepted Article

water line, 12 thermistors (Aanderaa in water depth > 22.7 m) at nominal depths of 6.5, 10.5, 14.5, 22.7, 26.1, 29.5, 32.9, 36.3, 39.7, 43.1, 46.5 and 49.9 m, and 2 current meters (InterOcean S4) at 17 and 53 m. After May 2006, the mooring was reconfigured and 13 AQUATEC temperature loggers were installed at 4 m intervals from around 1 m above sea floor to 16 m from the surface, including a CTD (Conductivity-Temperature-Depth) moored 11 m above see floor and a pressure sensor at the uppermost thermistor. Data were recorded every 5 min but all high-frequency moored measurements were averaged daily (including PH100).

Finally, we use local wind measurements from the Kurnell meteorological station (34.00^{o}S, 151.21^{o}E), recorded every 30 min since 1990, provided by the Australian Bureau of Meteorology. Wind stress (computed following *Schaeffer et al.* [2014]) was daily averaged, and low-passed using a Butterworth filter with a cut-off frequency of 24 h, before calculating an upwelling index as $UI = \frac{\tau_y}{\rho_0 |f|}$, where τ_y is the along-shelf wind stress (based on a 25 degree angle corresponding to the coastline rotation), $\rho_0 = 1025$ kg m^{-3}, the seawater density and f is the local Coriolis parameter.

2.2. Method: MHW definition and identification

Using the long-term in situ temperature datasets, we can investigate daily temperature anomalies below the ocean surface, by referencing a seasonally-varying climatology. We identify MHW events using the hierarchical approach defined by *Hobday et al.* [2016] in which time-series of temperature anomalies are calculated by subtracting a long-term (ideally 30 year) daily climatology of the 90th percentile temperature. A MHW event is defined when the warm temperature anomaly lasts for at least 5 days. Two events with a gap of 2 days or less are considered to be part of the the same event. We then investigate

©2017 American Geophysical Union. All Rights Reserved.

Accepted Article

various characteristics of the MHW, including their duration and intensity, defined as the temperature anomaly from the mean climatology. A few analysis were also perfomed for events longer than 10 days only, and the sensitivity of the duration threshold is discussed in last section.

To compute the daily temperature climatology we use all available data at each site, provided that 1) the samples were within <10 km from the site (based on a minimum length scale of variability in the region of 14km, *Schaeffer et al.* [2016a]) and 2) they were obtained in similar water depths (<110 m at PH100). Each vertical profile (from bottle samples, CTD casts or moorings) is linearly interpolated over depth at 1 m resolution, using pressure measurements when available, or nominal depths otherwise. Temperature data from the mooring array are used when data return exceeds 70% through the water column. In addition, gaps of ≥2 neighbouring thermistors are not interpolated. For each day of the year, the climatological mean and high percentile threshold (90th) are determined from a moving average over a window of +/- 5 days. Daily climatological time-series are then smoothed with a 31-day moving window following the procedure described in *Hobday et al.* [2016].

The identification of MHWs requires continuous daily temperature time-series, thus we only use periods when moorings were installed. At ORS065 we use data from 1992-2016 to compute both the climatology and warm temperature anomalies for depths 17-53 m (0-53 m until 2006). However the detection of MHWs at PH100 was limited to depths 25-100 m and starting in 2010 when the mooring was installed, while the climatology was computed from the bottle temperature observations between 1953-2016 (including mooring measurements, Fig. 1b). MHW events were identified independently at 5 m

©2017 American Geophysical Union. All Rights Reserved.

Accepted Article

depth intervals, as well as for the shallowest and deepest time-series at ORS065, at 1 and 53 m.

3. Results

3.1. MHW characteristics

A total of 38-50 MHW events were identified in 20-53 m of water at ORS065 over the period 1992-2016, and 24-27 events in 1-15 m when the mooring had a surface expression (1992-2006). Due to the shorter period available with daily temperature observations at PH100 (2010-2016), only 15-27 events were identified between 25 and 100 m depth. When averaging per year without considering days when observations are missing (more gaps in ORS065 dataset), we find an average of 17 -27 MHWs days per year, consistent at both sites (Fig. 2a).

The mean temperature anomaly is a maximum of 2.55 ^{o}C at 50 m depth at both sites, decreasing to 1.8 ^{o}C towards the surface at ORS065 and towards the ocean floor at PH100 (2.1 ^{o}C at 100 m depth, Fig. 2b). The greatest temperature anomaly over all events was 5.7-6^{o}C at depth at both sites. On average, MHWs lasted between 8-11 and 9-12 days at PH100 and ORS065 respectively (Fig. 2c). However the variability was greater at ORS065 (higher standard deviations) due to the longer time-series over which MHWs are detected. The longest event at PH100 occurred in September 2015 for 24 days at 30 m depth, with a previous event of a week just 4 days before. The event was identified over the whole water column, but was of longer duration at the surface. Taking into account times back to 1992 at ORS065, July 2001 was characterized by the longest event, lasting more than a month at all depths, up to 52 days close to the bottom.

Accepted Article

©2017 American Geophysical Union. All Rights Reserved.

3.2. Depth extent of MHWs

More than half of the MHW events identified at 20 m depth at ORS065 were also observed at the deepest temperature record (53 m depth in water depth of 60-65m). At PH100, only a third of the events occurring at 25 m were observed to reach the near bottom (depths >85 m), due to the midshelf location and greater depth. These events were longer than shallow events, with a mean duration of 16 days compared to 8 days at 20 m at ORS065, 9 days compared to 8 days at 25 m at PH100 (not shown). In addition, the events spanned all seasons (Fig. 3a,d). However, the vertical profiles of temperature show a more homogeneous water column during the deep events compared to the shallow ones. Events constrained to the SML often correspond to temperature profiles marked by an intense thermocline (dashed lines in Fig. 3a,d). This is confirmed when extracting a stratification index (temperature difference between depths of 20 and 53 m at ORS065, 25 and 80 m at PH100) during each event identified at each depth (Fig. 3b,e). MHWs at depth tend to occur when the stratification is weak. The mean stratification during the deepest MHWs is 0.9 ^{o}C at ORS065 and 1.5 ^{o}C at PH100, compared to an average of 3.2^{o}C and 5 ^{o}C during shallow events (Fig. 3b,e).

Since deep MHW events occur during weak stratification but are not seasonal (they also occur during summer, Fig. 3a,d), we expect vertical mixing to drive the weak stratification and enable MHWs to extend deeper than the SML. Figures 3c,f show the averaged wind conditions during the MHWs, as well as during the onset or decline of the events. In the region, wind direction is usually from the south [*Rossi et al.*, 2014; *Wood et al.*, 2012], downwelling favorable, as shown by the negative averaged upwelling index (UI) over the whole time period, shown as reference (black dots in Fig. 3c,f). We also calculate

©2017 American Geophysical Union. All Rights Reserved.

Accepted Article

a composite UI during the events, i.e. we identify the upwelling index over the whole event (average), and at their start and end (by depth) and create a composite UI from all the events at every depth, from which we calculate the mean and standard deviation of the UI. Fig. 3c,f show that the composite UI is more negative (indicating downwelling) during MHWs, especially during the onset of the events. Moreover, the deeper MHWs are associated with a more negative UI (indicated by the slope of the UI onset curve, being more negative with depth). This suggests that local downwelling favorable winds enhance vertical mixing and enable the warming of deeper waters, driving extreme temperature anomalies. In contrast, wind conditions at the end of MHWs are weaker and more upwelling-favorable than the reference, suggesting that upwelling can suppress the warm water event. An example of the effect of wind forcing on the temperature anomaly over time is presented in Fig. S1, showing strong upwelling winds before and after the MHW, but downwelling-favorable wind stress at the onset of the event.

3.3. Variability of intensity

The intensity of MHWs is one of the key characteristics impacting the local marine environment. Despite exhibiting high variability, there is a strong seasonal signal in intensity of the warm temperature anomalies during the events (Fig. 4a,b). This is consistent with the climatological annual cycle [*Wood et al.*, 2016], with the greatest intensities occurring in summer, in particular January-February, with a high variability between events, ranging 1.6-4.9 ^{o}C. This contrasts with winter conditions (June-August), when the greatest mean MHW intensity observed is < 2.3 ^{o}C.

Monthly composite values at each depth highlight the vertical variability of this seasonal cycle. In contrast to the absolute temperature during MHWs (Fig. S2), the most

©2017 American Geophysical Union. All Rights Reserved.

Accepted Article

pronounced seasonal cycle of their intensity (referred to the climatology) occurs at depth rather than at the surface (Fig.4c,d). More precisely, MHWs occur at the greatest intensities at depths of 30-70 m at both sites, with the warmest temperature anomalies exceeding 4 ^{o}C on average in February (Fig.4c,d). This sub-surface maximum is located just below the maximum variance of temperature (Fig. 4e,f), matching the location of the thermocline. Because of the strong vertical gradient in temperature, when the water mass above the thermocline is downwelled to greater depth, the temperature anomaly is a maximum. Similarly, we expect cold events to be the most intense just above the thermocline (not shown).

4. Discussion and conclusions

We have examined MHWs at two sites on the continental shelf of SE Australia using long-term (7 years and 25 years) in situ temperature measurements down to 100 m deep, based on a climatology spanning 1953-2016 and 1992-2016, respectively. We found that MHWs below the surface occur all year long, with an average intensity of 1.8-2.5 ^{o}C and duration of 8-12 days. For the first time to our knowledge, we show that MHWs regularly extend to the bottom of the water column, and are driven by downwelling favorable winds during periods of weak stratification. It should be noted that we find similar results when focusing only on events longer than 10 days (compared to a threshold of 5 days defined by *Hobday et al.* [2016], see Figs. 2b, 3c,f and 4a,b), but we expect large scale processes (such as anomalous air-sea heat fluxes and ocean advection) to be a major driver of long record events, in agreement with the findings of *Chen et al.* [2015]; *Bond et al.* [2015]; *Benthuysen et al.* [2014] in other regions.

©2017 American Geophysical Union. All Rights Reserved.

Accepted Article

In addition to changes in regional oceanography (e.g. *Oliver et al.* [2014]), we show that understanding how coastal wind forcing may change in the future is of great importance for MHWs. Future projections along the SE coast of Australia suggest a decrease of downwelling favorable winds (*Sen Gupta et al.* [2016], Fig S5). This might lead to shallower MHWs, while local persistent upwelling [*Loureno et al.*, 2016] or intrusive bottom uplift [*Benthuysen et al.*, 2016] could provide respite from ocean warming and new habitat for some species.

Coastal margins are where a significant part of the global productivity occurs [*Pomeroy*, 1974] thus this is where maximum ecosystem damage will occur due to the relative shallow depths (< 200 m). The intensity of MHWs, or how much warmer the ocean is compared to a seasonally-varying average, is of particular interest since most organisms have a preferable temperature range and physiological thermal threshold [*O'Connor et al.*, 2007]. We found that extreme temperature anomalies are greatest at the end of summer and that the intensity of MHWs is greatest at depth, just below the maximum variance of temperature (thermocline). This sub surface intensity maximum is in agreement with previously observed heat damage to benthic species, such as coral, kelp and seagrass [*Poloczanska et al.*, 2007; *Wernberg et al.*, 2013; *Marzinelli et al.*, 2015; *Thomson et al.*, 2015]. In addition, we can expect an influence of these extreme temperature anomalies on phytoplankton growth, as the deep chlorophyll-a maximum is often observed around the depth of greatest MHW intensity (e.g. *Schaeffer et al.* [2016b]) and the time-scale required for phytoplankton to double their size is of the same order as the duration of MHW events (days, *Denman et al.* [2003]). While the direct effect of temperature on phytoplankton productivity is still under debate, most studies agree on a significant thermal influence

©2017 American Geophysical Union. All Rights Reserved.

Accepted Article

when no other factor is limiting (e.g. nutrients and light) [*Huertas et al.*, 2011; *Edwards et al.*, 2016].

Our study highlights an urgent need for long-term sustainable sub-surface temperature observations. While satellite SST is incontestably a very valuable tool for studying large scale temperature extremes, we showed that the surface information does not represent the deeper signature of MHWs. Some events even only occur at depth and would not be detected using surface temperature time-series (e.g. Fig. S1). Moreover, gaps in the spatial and temporal coverage (due to clouds) can lead to an underestimation of the intensity and duration of the MHW events. For example it was shown that satellite SST underestimated the peak of the massive coral bleaching that occurred in 2016 on the Great Barrier Reef (Greg Steinberg, pers. com., February 2017). Understanding MHWs is a necessary step for better management of our ecosystems [*Johnson*, 2014] and we show that their depth extent also matters.

Finally, our findings emphasize the need to take into account regional dynamics in coastal regions. While additonal long-term in situ observations are not available to explore the spatial extent of deep MHWs, we expect the intensity of MHWs to be maximum in summer below the surface in all seasonally-stratified oceans. We also show that local wind stress, which is a major driver of coastal circulation in continental shelf and coastal regions [*Lentz*, 2008; *Gong and Glenn*, 2010], should be taken into account to understand the onset and decline of MHWs where upwelling-downwelling processes occur. Therefore we believe our conclusions are relevant for coastal regions globally.

Acknowledgments. PH100 data was sourced from the Integrated Marine Observing System (IMOS). IMOS is a national collaborative research infrastructure, supported by

©2017 American Geophysical Union. All Rights Reserved.

Accepted Article

the Australian Government. All data is freely available at www.aodn.org.au. We are very grateful to C. Holden (Oceanographic Field Services Pty Ltd) and Sydney Water Corporation for the ongoing collection of ORS065 data. We acknowledge everyone who has been involved in field work since 1953 and the foresight of CSIRO Marine Research for instigating and continuing the data collection. In addition we thank T. Ingleton and B. Morris, NSW Office of Environment and Heritage, as well as T. Austin and G. Galibert for data processing. Some of the code used to perform this analysis was adapted from the *MarineHeatWaves* module for python that was written and made publicly available by E. Oliver (https://github.com/ecjoliver/marineHeatWaves).

Accepted Article

©2017 American Geophysical Union. All Rights Reserved.

Accepted Article

References

Benthuysen, J., M. Feng, and L. Zhong (2014), Spatial patterns of warming off Western Australia during the 2011 Ningaloo Nio: Quantifying impacts of remote and local forcing, *Continental Shelf Research*, *91*, 232 – 246, doi:http://dx.doi.org/10.1016/j.csr.2014.09.014.

Benthuysen, J. A., H. Tonin, R. Brinkman, M. Herzfeld, and C. Steinberg (2016), Intrusive upwelling in the central Great Barrier Reef, *Journal of Geophysical Research: Oceans*, *121*(11), 8395–8416, doi:10.1002/2016JC012294.

Bond, N. A., M. F. Cronin, H. Freeland, and N. Mantua (2015), Causes and impacts of the 2014 warm anomaly in the NE Pacific, *Geophysical Research Letters*, *42*(9), 3414–3420, doi:10.1002/2015GL063306, 2015GL063306.

Cai, W., G. Shi, T. Cowan, D. Bi, and J. Ribbe (2005), The response of the southern annular mode, the East Australian Current, and the southern mid-latitude ocean circulation to global warming, *Geophysical Research Letters*, *32*(23), doi:10.1029/2005GL024701.

Chen, K., G. Gawarkiewicz, Y.-O. Kwon, and W. G. Zhang (2015), The role of atmospheric forcing versus ocean advection during the extreme warming of the northeast U.S. continental shelf in 2012, *Journal of Geophysical Research: Oceans*, *120*(6), 4324–4339, doi:10.1002/2014JC010547.

Denman, K.L., and D.M Powell (2003): Chapter 4 - Effects of physical processes on planktonic ecosystems in the coastal ocean. *Oceanography and Marine Biology - An Annual Review*, H. Branes, Eds., Taylor & Francis, 116 – 163.

Edwards, K. F., M. K. Thomas, C. A. Klausmeier, and E. Litchman (2016), Phytoplankton growth and the interaction of light and temperature: A synthesis at the

©2017 American Geophysical Union. All Rights Reserved.

species and community level, *Limnology and Oceanography*, *61*(4), 1232–1244, doi: 10.1002/lno.10282.

Feng, M., M. J. McPhaden, S.-P. Xie, and J. Hafner (2013), La Nia forces unprecedented Leeuwin Current warming in 2011, *Nature Scientific Reports*, *3*(1277), doi:http://dx.doi.org/10.1038/srep01277.

Gong, J. T. K., D., and S. M. Glenn (2010), Seasonal climatology of wind-driven circulation on the New Jersey shelf, *J. Geophys. Res.*, *115*, C04,006, doi:doi:10.1029/2009JC005520.

Hobday, A. J., L. V. Alexander, S. E. Perkins, D. A. Smale, S. C. Straub, E. C. Oliver, J. A. Benthuysen, M. T. Burrows, M. G. Donat, M. Feng, N. J. Holbrook, P. J. Moore, H. A. Scannell, A. S. Gupta, and T. Wernberg (2016), A hierarchical approach to defining marine heatwaves, *Progress in Oceanography*, *141*, 227 – 238, doi:http://dx.doi.org/10.1016/j.pocean.2015.12.014.

Huertas, I. E., M. Rouco, V. López-Rodas, and E. Costas (2011), Warming will affect phytoplankton differently: evidence through a mechanistic approach, *Proceedings of the Royal Society of London B: Biological Sciences*, doi:10.1098/rspb.2011.0160.

Johnson, C. R., S. C. Banks, N. S. Barrett, F. Cazassus, P. K. Dunstan, G. J. Edgar, S. D. Frusher, C. Gardner, M. Haddon, F. Helidoniotis, K. L. Hill, N. J. Holbrook, G. W. Hosie, P. R. Last, S. D. Ling, J. Melbourne-Thomas, K. Miller, G. T. Pecl, A. J. Richardson, K. R. Ridgway, S. R. Rintoul, D. A. Ritz, D. J. Ross, J. C. Sanderson, S. A. Shepherd, A. Slotwinski, K. M. Swadling, and N. Taw (2011), Climate change cascades: Shifts in oceanography, species' ranges and subtidal marine community dynamics in eastern Tasmania, *Journal of Experimental Marine Biology and Ecology*, *400*(12), 17 –

Accepted Article

©2017 American Geophysical Union. All Rights Reserved.

32, doi:http://dx.doi.org/10.1016/j.jembe.2011.02.032, global change in marine ecosystems.

Johnson, N., J.E.and Holbrook (2014), Adaptation of Australia's marine ecosystems to climate change: Using science to inform conservation management, *International Journal of Ecology, 2014*, doi:10.1155/2014/140354.

Last, P. R., W. T. White, D. C. Gledhill, A. J. Hobday, R. Brown, G. J. Edgar, and G. Pecl (2011), Long-term shifts in abundance and distribution of a temperate fish fauna: a response to climate change and fishing practices, *Global Ecology and Biogeography, 20*(1), 58–72, doi:10.1111/j.1466-8238.2010.00575.x.

Lentz, S. J. (2008), Seasonal Variations in the Circulation over the Middle Atlantic Bight Continental Shelf., *J. Phys. Oceanogr., 38*, 14861500, doi:http://dx.doi.org/10.1175/2007JPO3767.1.

Lima, F., and D. Wethey (2012), Three decades of high-resolution coastal sea surface temperatures reveal more than warming, *Nature Communications, 3*, 1–13, doi:http://dx.doi.org/10.1038/ncomms1713.

Ling, S. D., C. R. Johnson, K. Ridgway, A. J. Hobday, and M. Haddon (2009), Climate-driven range extension of a sea urchin: inferring future trends by analysis of recent population dynamics, *Global Change Biology, 15*(3), 719–731, doi:10.1111/j.1365-2486.2008.01734.x.

Loureno, C. R., G. I. Zardi, C. D. McQuaid, E. A. Serro, G. A. Pearson, R. Jacinto, and K. R. Nicastro (2016), Upwelling areas as climate change refugia for the distribution and genetic diversity of a marine macroalga, *Journal of Biogeography, 43*(8), 1595–1607, doi:10.1111/jbi.12744.

©2017 American Geophysical Union. All Rights Reserved.

Accepted Article

Lynch, T. P., E. B. Morello, K. Evans, A. J. Richardson, W. Rochester, C. R. Steinberg, M. Roughan, P. Thompson, J. F. Middleton, M. Feng, R. Sherrington, V. Brando, B. Tilbrook, K. Ridgway, S. Allen, P. Doherty, K. Hill, and T. C. Moltmann (2014), IMOS national reference stations: A continental-wide physical, chemical and biological coastal observing system, *PLOS ONE*, *9*(12), 1–28, doi:10.1371/journal.pone.0113652.

Marzinelli, E., S. Williams, R. Babcock, N. Barrett, C. Johnson, A. Jordan, G. Kendrick, O. Pizarro, D. Smale, and P. Steinberg (2015), Large-scale geographic variation in distribution and abundance of Australian deep-water kelp forests, *PLoS ONE*, *10*(2), doi:10.1371/journal.pone.0118390.

O'Connor, M., Bruno J.F., Gaines S.D., Halpern B.S., Lester S.E., Kinlan B.P., and Weiss J.M. (2007), Temperature control of larval dispersal and the implications for marine ecology, evolution, and conservation., *Proc Natl Acad Sci*, *104(4)*, 1266–1271.

Oliver, E. C. J., S. J. Wotherspoon, M. A. Chamberlain, and N. J. Holbrook (2014), Projected Tasman sea extremes in sea surface temperature through the twenty-first century, *Journal of Climate*, *27*(5), 1980–1998, doi:10.1175/JCLI-D-13-00259.1.

Pearce, A. F., and M. Feng (2013), The rise and fall of the marine heat wave off Western Australia during the summer of 2010/2011, *Journal of Marine Systems*, *111112*, 139 – 156, doi:10.1016/j.jmarsys.2012.10.009.

Poloczanska, E. S., R. C. Babcock, A. Butler, A. Hobday, O. Hoegh-Guldberg, T. J. Kunz, R. Matear, D. A. Milton, T. A. Okey, and A. J. Richardson (2007), Climate change and Australian marine life, in *Oceanography And Marine Biology*, vol. 45, edited by Gibson, RN and Atkinson, RJA and Gordon, JDM, pp. 407–478.

Accepted Article

©2017 American Geophysical Union. All Rights Reserved.

Pomeroy, L. R. (1974), The ocean's food web, a changing paradigm, *BioScience*, *24*(9), 499, doi:10.2307/1296885.

Rossi, V., A. Schaeffer, J. Wood, G. Galibert, B. Morris, J. Sudre, M. Roughan, and A. M. Waite (2014), Seasonality of sporadic physical processes driving temperature and nutrient high-frequency variability in the coastal ocean off southeast Australia, *Journal of Geophysical Research: Oceans*, *119*(1), 445–460, doi:10.1002/2013JC009284.

Roughan, M., A. Schaeffer, and I. M. Suthers, 2015: Chapter 6 - sustained ocean observing along the coast of southeastern Australia: NSW-IMOS 20072014. *Coastal Ocean Observing Systems*, Y. Liu, H. Kerkering, and R. H. Weisberg, Eds., Academic Press, Boston, 76 – 98, doi:10.1016/B978-0-12-802022-7.00006-7.

Scannell, H. A.,A. J. Pershing,M. A. Alexander,A. C. Thomas, andK. E. Mills (2016), Frequency of marine heatwaves in the North Atlantic and North Pacific since 1950, *Geophys. Res. Lett.*, *43*, 2069 – 2076, doi:10.1002/2015GL067308.

Schaeffer, A., M. Roughan, and B. Morris (2013), Cross-shelf dynamics in a western boundary current. Implications for upwelling., *Journal of Physical Oceanography*, *43*, 1042 – 1059, doi:http://dx.doi.org/10.1175/JPO-D-12-0177.1.

Schaeffer, A., M. Roughan, and B. Morris (2014b), Corrigendum cross-shelf dynamics in a western boundary current. Implications for upwelling., *Journal of Physical Oceanography*, *44*, 28122813, doi:http://dx.doi.org/10.1175/JPO-D-14-0091.1.

Schaeffer, A., M. Roughan, and J. E. Wood (2014), Observed bottom boundary layer transport and uplift on the continental shelf adjacent to a western boundary current, *Journal of Geophysical Research: Oceans*, *119*, 4922 – 4939, doi:10.1002/2013JC009735.

Accepted Article

©2017 American Geophysical Union. All Rights Reserved.

Schaeffer, A., M. Roughan, D. White, and E. Jones (2016a), Physical and biogeochemical spatial scales of variability in the East Australian Current separation zone from shelf glider measurements, *Biogeosciences*, *13*, doi:10.5194/bg-13-1967-2016.

Schaeffer, A., M. Roughan, T. Austin, J. D. Everett, D. Griffin, B. Hollings, E. King, A. Mantovanelli, S. Milburn, B. Pasquer, C. Pattiaratchi, R. Robertson, D. Stanley, I. Suthers, and D. White (2016b), Mean hydrography on the continental shelf from 26 repeat glider deployments along southeastern Australia, *Scientific Data*, *3*, 160,070, doi:10.1038/sdata.2016.70.

Sen Gupta, A., J. Brown, N. Jourdain, E. van Sebille, A. Ganachaud, and A. Verges (2015), Episodic and non-uniform shifts of thermal habitats in a warming ocean, *Deep-Sea Research Part II: Topical Studies in Oceanography*, *113*, 59–72, doi:10.1016/j.dsr2.2013.12.002.

Sen Gupta, A., S. McGregor, E. van Sebille, A. Ganachaud, J. N. Brown, and A. Santoso (2016), Future changes to the Indonesian Throughflow and pacific circulation: The differing role of wind and deep circulation changes, *Geophysical Research Letters*, *43*(4), 1669–1678, doi:10.1002/2016GL067757, 2016GL067757.

Thompson, P., M. Baird, T. Ingleton, and M. Doblin (2009), Long-term changes in temperate Australian coastal waters: Implications for phytoplankton, *Marine Ecology Progress Series*, *394*, 1–19.

Thomson, J., D. d. Burkholder, M. Heithaus, J. Fourqurean, M. Fraser, J. c. Statton, and G. Kendrick (2015), Extreme temperatures, foundation species, and abrupt ecosystem change: an example from an iconic seagrass ecosystem, *Global Change Biology*, *21*(4), 1463–1474, doi:10.1111/gcb.12694.

©2017 American Geophysical Union. All Rights Reserved.

Accepted Article

Verges, A., C. Doropoulos, H. Malcolm, M. Skye, M. Garcia-Piz, E. Marzinelli, A. Campbell, E. Ballesteros, A. Hoey, A. Vila-Concejo, Y.-M. Bozec, and P. Steinberg (2016), Long-term empirical evidence of ocean warming leading to tropicalization of fish communities, increased herbivory, and loss of kelp., *Proc Natl Acad Sci*, *113*(48), 13,791–13,796, doi:10.1073/pnas.1610725113.

Wernberg, T., D. A. Smale, F. Tuya, M. S. Thomsen, T. J. Langlois, T. De Bettignies, S. Bennett, and C. S. Rousseaux (2013), An extreme climatic event alters marine ecosystem structure in a global biodiversity hotspot, *Nature Climate Change*, *3*(1), 78–82.

Wernberg, T., S. Bennett, R. C. Babcock, T. de Bettignies, K. Cure, M. Depczynski, F. Dufois, J. Fromont, C. J. Fulton, R. K. Hovey, E. S. Harvey, T. H. Holmes, G. A. Kendrick, B. Radford, J. Santana-Garcon, B. J. Saunders, D. A. Smale, M. S. Thomsen, C. A. Tuckett, F. Tuya, M. A. Vanderklift, and S. Wilson (2016), Climate-driven regime shift of a temperate marine ecosystem, *Science*, *353*(6295), 169–172, doi:10.1126/science.aad8745.

Wood, J., M. Roughan, and P. Tate (2012), Finding a proxy for wind stress over the coastal ocean, *Marine and Freshwater Research*, *63*, 528544.

Wood, J., A. Schaeffer, M. Roughan, and P. Tate (2016), Seasonal variability in the continental shelf waters off southeastern Australia: Fact or fiction?, *Continental Shelf Research*, *112*, 92 – 103, doi:http://dx.doi.org/10.1016/j.csr.2015.11.006.

Wu, L., W. Cai, L. Zhang, H. Nakamura, A. Timmermann, T. Joyce, M. J. McPhaden, M. Alexander, B. Qiu, M. Visbeck, P. Chang, and B. Giese (2012), Enhanced warming over the global subtropical western boundary currents, *Nature Climate Change*, *2, Issue 3*, 161–166.

Accepted Article

©2017 American Geophysical Union. All Rights Reserved.

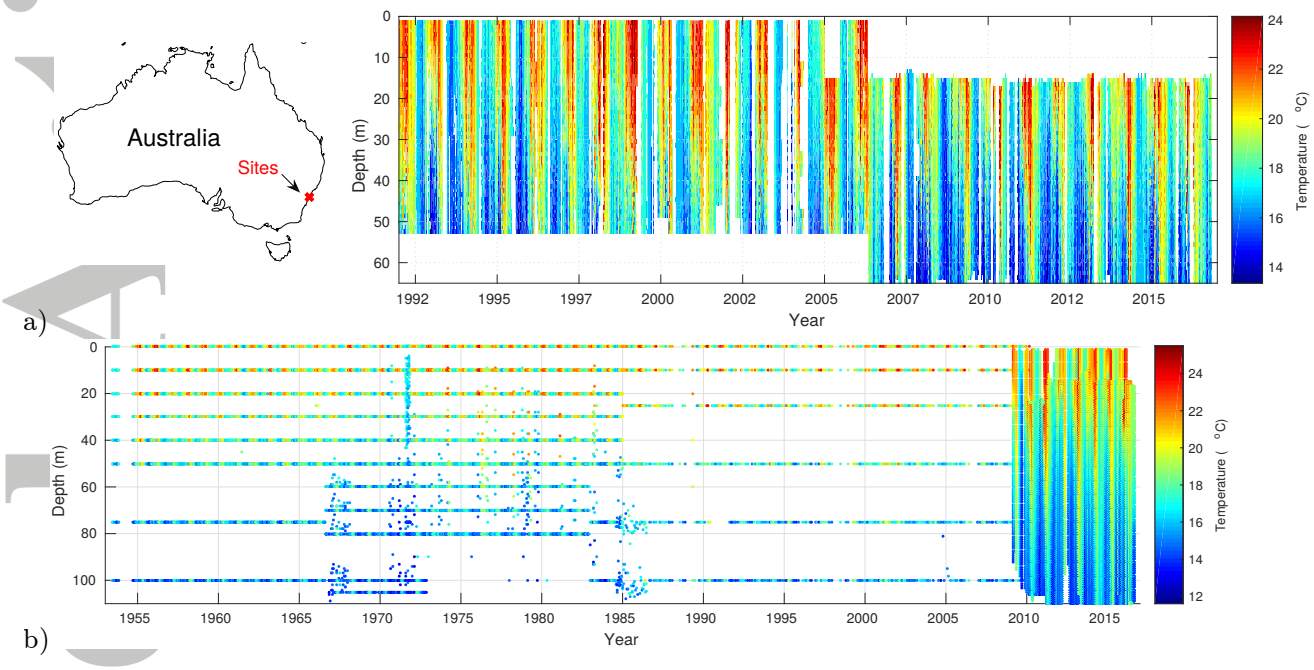

Figure 1. Temperature measurements at ORS065 (a), PH100 (b). The inset shows the location of the two sites, 25 km apart on the east coast of Australia at ∼34°S. A local map is available in Roughan et al. [2015].

©2017 American Geophysical Union. All Rights Reserved.

Accepted Article

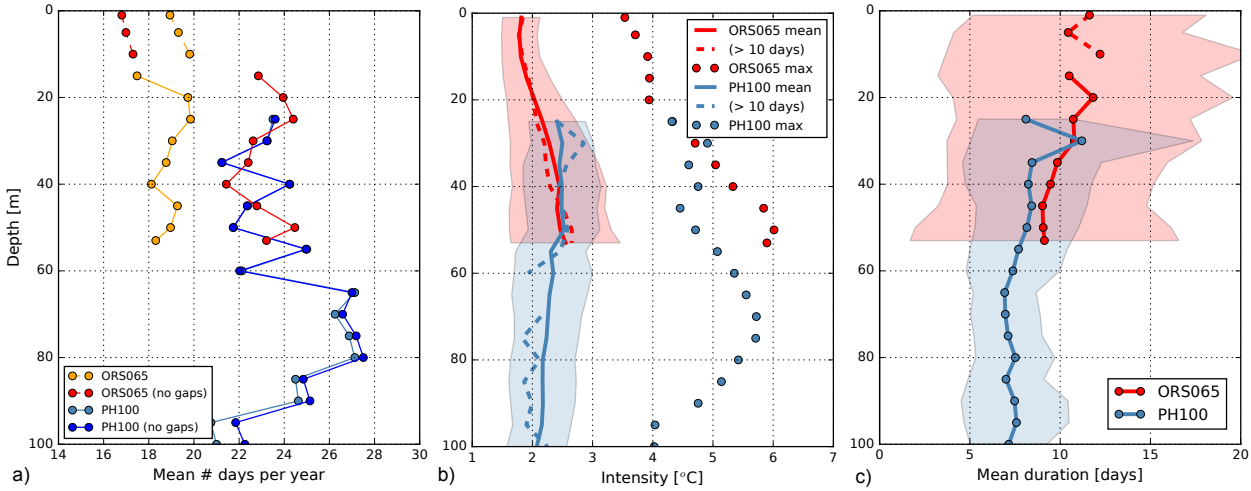

Figure 2. Characteristics of MHW events over depth: a) mean MHW days per year ("no gaps" refers to the mean calculated based only on days when data was available, for example if 20 MHW days were detected over a year with only 200 days of good data, i.e. 10%, it is equivalent to 36 MHW days over the year), b) mean intensity and maximum over all events, c) mean duration. Shadings show the standard deviation over events. Dashed lines in b) show means for longer events (>10 days).

©2017 American Geophysical Union. All Rights Reserved.

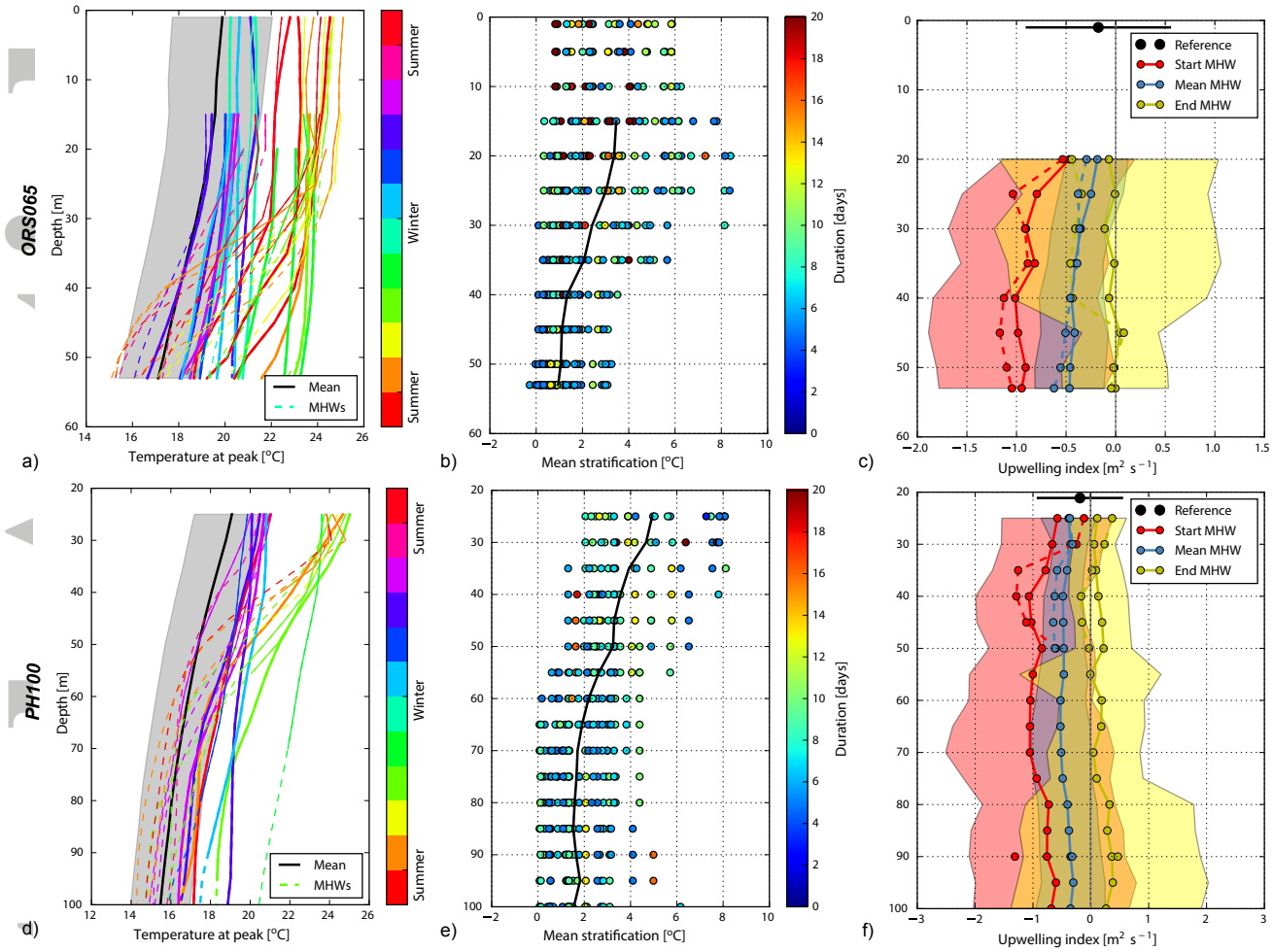

Figure 3. a,d) Vertical profile of temperature: mean and standard deviation over the whole time-series (black line and shading) and instantaneous profile at the peak of each MHW event identified at sub-surface (20 m at ORS065 and 25 m at PH100), colored by month (referred to austral summer and winter). Dashed lines are overlaid by solid lines from the sub-surface until the maximum depth where the MHW was identified. Bold lines show the events that reached the bottom boundary layers (within 15 m of the bottom). b,e) Mean stratification for every event identified at every depth, colored by duration of the event. The black line shows the average over all events for each depth. c,f) Composite of the upwelling index calculated from the wind stress during every event at every depth. Means and standard deviations are computed from all MHW events, based on their start day (red), end day (yellow) and whole duration (blue). Black dot and line at the top of the panel indicate the mean and standard deviations over the whole time-series independent of MHWs. For all panels, first row is for ORS065 and second for PH100 site. Dashed lines in c) and f) show composites for longer events (>10 days).

©2017 American Geophysical Union. All Rights Reserved.

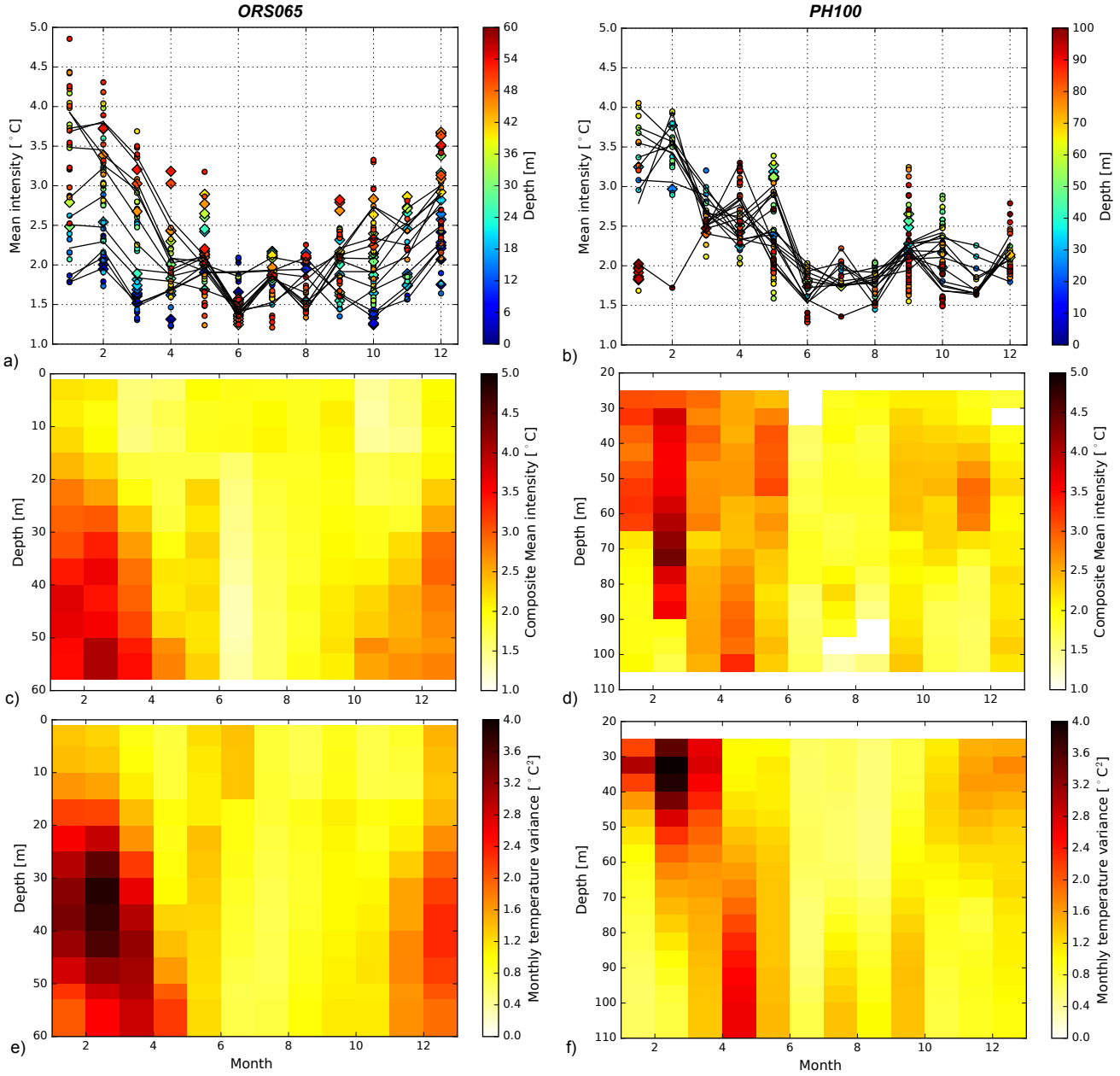

Figure 4. Mean intensity of MHW events as a function of their start month at ORS065 (a) and PH100 (b). Colors show the depth of the event, solid lines link the composite values for each depth and month. Diamonds refer to long events (>10 days). Composite mean intensity during MHWs binned by depth and month at ORS065 (c) and PH100 (d). White cells show depths and months with no events. Temperature variance over the climatological period binned by depth and months at ORS065 (e) and PH100 (f).

©2017 American Geophysical Union. All Rights Reserved.

Accepted